

Chirped Frequency Conversion in Optical Parametric Devices for Reducing Speckle in Active Imaging Applications at 1550nm

Karl A. Tillman and Derryck T. Reid

Ultrafast Optics Group, School of Engineering and Physical Sciences
Heriot-Watt University, Edinburgh, EH14 4AS, UK
<http://www.phy.hw.ac.uk/resrev/ufast/>

Abstract

We describe the development of microjoule energy broadband parametric sources operating at 1.5 μ m and compatible with burst-illumination imaging. Four quasi-phasematched devices, all based on 50mm long crystals of magnesium-doped (5%) periodically poled lithium niobate (MgO:PPLN), were compared in terms of their output pulse energy and bandwidth. The first was a CW-seeded optical parametric amplifier (OPA) and was a control experiment. Two other devices were OPAs using different seeds / gratings to increase the output bandwidth while the final device was a multi-grating aperiodically-poled OPO.

Keywords: Burst illumination imaging, optical parametric amplification, aperiodically poled, quasi-phasematching, MgO:PPLN, fan-out grating

1. Introduction

Laser sources suitable for free-space ranging and imaging applications must possess high pulse energies and repetition rates in addition to operating at a wavelength compatible with atmospheric transmission. The beam quality of these sources should also be very close to diffraction limited which is only possible by using a diffraction limited pump source. This project has been concerned with the development of optical parametric devices (amplifiers and oscillators) that meet these criteria and are based on an actively Q-switched configuration operated at 1.5 μ m.

One important criterion for sources intended for free-space propagation is often the need for optical pulses with a short coherence length as this leads to more accurate ranging and in imaging applications a reduction in laser speckle effects. The inverse relationship between the coherence length and the spectral bandwidth of an illuminating pulse means that to produce a short coherence length a

broadband spectrum is required. In optical parametric devices (OPAs and OPOs) the spectral bandwidth is determined by the conversion bandwidth of the nonlinear crystal and (OPAs only) the bandwidth of the seed spectrum. An OPO is self-seeded by quantum noise [1] and it is the bandwidth of the optical parametric fluorescence (OPF) spectrum which acts as a seed with the cavity mirror coatings determining the range of resonant wavelengths. In an OPA a pump source is used to amplify an external seed source and, provided the crystal is capable of generating an OPF signal to match the seed bandwidth, amplification of the entire seed spectrum occurs. Broad spectral bandwidths can readily be found in femtosecond lasers such as an erbium-doped fibre laser. In previous work (Tillman et al [2]) a new method of optical parametric amplification was demonstrated in which an aperiodically-poled (chirped) QPM crystal was used to obtain broadband optical parametric oscillation using stretched pump pulses from a femtosecond laser. The same

approach can be used to construct an OPO or OPA pumped by narrowband high-energy Q-switched pulses and, in the case of an OPA, seeded by broadband highly chirped femtosecond pulses.

Conventionally, OPAs have used either birefringently phase-matched or periodically-poled QPM crystals which have an associated gain bandwidth that varies inversely with crystal length. Using the conventional approach it is therefore difficult to simultaneously achieve high gain (implying a long crystal) and broad conversion bandwidth (implying a short crystal). These mutually exclusive conditions can fortunately be met simultaneously by using a QPM crystal whose grating period is aperiodic [2]. Modern electric-field poling techniques make it possible to realise several different types of aperiodic QPM grating structures that are suitable for broadband parametric amplification. The most commonly used aperiodic QPM grating structure is one whose period varies linearly along the direction of propagation (axially chirped).

seed using either a axially chirped (b) or a laterally chirped crystal (c) in a QPM OPA.

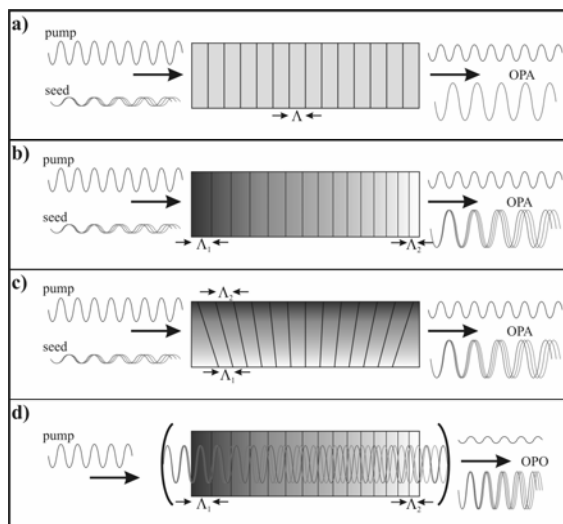


Fig.1: Concept of (a) conventional, (b) axially chirped, and (c) laterally chirped OPAs, and (d) a axially chirped OPO

Similarly, Figure 1 (d) shows how a axially chirped crystal placed within an OPO

This grating structure can be viewed as many short gain regions stacked end-to-end so different frequencies see gain at different axially separated locations. As a result the gain-per-unit-frequency is limited to a section of the total crystal length with all of the converted frequencies following the same path through the crystal. An alternative approach is to use a QPM grating whose period varies laterally across the crystal (laterally chirped or fan-out grating) [3]. This structure can be viewed as many thin gain regions stacked top-to-bottom allowing different frequencies to see gain at different laterally spaced locations. This approach allows the maximum possible gain-per-unit-frequency (i.e. the entire crystal length) but each generated frequency follows a different path through the crystal. The lateral approach therefore has the potential to generate higher energy output pulses than the axially approach but at the cost of increased system complexity.

Figure 1 illustrates how, in contrast to a conventional unchirped crystal (a), a narrow bandwidth pump can amplify a broadband cavity can be used to generate a broadband output.

The designs of the three OPAs were all based on a Q-switched Nd:YLF laser (Lightwave 110B) operating at 1kHz and producing 3.5ns pulses with energies of $\sim 110\mu\text{J}$. For broadband operation this laser pumped the OPA in synchronism with low-energy pulses from a femtosecond Er:fibre laser (Menlosystems, GmbH) centred at $\sim 1.55\mu\text{m}$ with a bandwidth in excess of 100nm. Figure 2 shows a schematic of one of the fs-seeded chirped OPAs. Prior to amplification the femtosecond seed pulses were stretched from $\sim 150\text{fs}$ to 3.5ns using 4.5km of SMF28 telecommunications fibre to duration match them with the pump pulses and maximum the potential for parametric gain. Synchronization between the two lasers was achieved by using a 54MHz radio-frequency oscillator onboard the Q-switched laser as a master oscillator to which the pulse repetition rate of the

Er:fibre laser was slaved. All four of the nonlinear crystals (HC-Photonics) were based on MgO:PPLN which has the same high gain of PPLN but exhibits photorefractivity of around 100 times less allowing it to operate at room temperature [4], giving access to a particularly broad temperature tuning range.

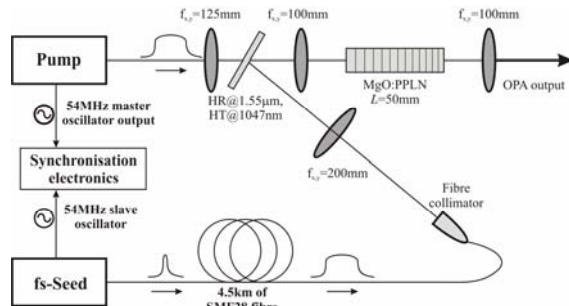


Fig.2: Schematic of the experimental setup used in the axially chirped OPA

One of the important design issues for all of the amplifiers was the need to maintain the pump intensities below the damage threshold for lithium niobate (50MWcm^{-1}) [5] while simultaneously satisfying the optimum parametric focusing condition [6]. In the case of the CW-seeded OPA a conservative elliptical focusing geometry was adopted to ensure operation below the damage threshold given by [5]. However for the axially chirped fs-seeded OPA the damage threshold was reassessed and the final focal configuration used higher intensity spherically focused pump/seed beams. For the laterally chirped fs-seeded OPA a significantly more complex geometry was needed to ensure that firstly the pump filled as much of the crystal aperture as possible and secondly that the component seed frequencies were focused into correct grating period of the crystal. For the OPO the focal considerations were based on optimising the mode-matching between the pump and resonant beams [6] below the reassessed damage threshold in MgO:PPLN of 1Jcm^{-1} .

The aim of developing the chirped-pulse OPAs was to compare the performance of femtosecond (fs) seeding with continuous-wave (CW) seeding and so quantify any

advantage to using a broadband femtosecond laser for bandwidth enhancement. For this reason three MgO:PPLN crystals were designed, the first used an unchirped $30.52\mu\text{m}$ period grating, the second used an axially chirped grating with periods varying from $30.0\text{--}30.7\mu\text{m}$ and the third used a laterally chirped grating with periods varying from $30.1\text{--}30.8\mu\text{m}$. The first device used the unchirped crystal and a narrow-line CW fibre laser operating at $1.553\mu\text{m}$ and is briefly summarised in Section 2 (for further details see the 1st EMRS-DTC annual conference proceedings). The second device used the axially chirped crystal and a broadband modelocked fs-seeded fibre laser and is briefly summarised in Section 3 (for further details see the 2nd EMRS-DTC annual conference proceedings). The third device involving the laterally chirped crystal and a broadband fs-seeded fibre laser is summarised in Section 4. The fourth device was an OPO based around a multi-grating crystal containing one unchirped grating with a period of $30.25\mu\text{m}$ and five axially chirped gratings with grating chirps ranging progressively from $0.01\mu\text{m}$ to $0.14\mu\text{m}$. The OPO is described in section 5 while section 6 draws some conclusions and discusses potential extensions.

2. CW-seeded OPA

The CW-OPA was intended as a benchmark with which to compare the performance of chirped devices, and its design used spherical 125mm and 200mm lenses respectively to collimate the beams from the pump laser and seed fibre collimator and a 63mm cylindrical lens to focus the pump and seed light into the MgO:PPLN crystal. After matching the two beam profiles to a model, developed using a simple ABCD propagation matrix program written using Matlab, a low-level parametric fluorescent signal was detected using a fast ($<175\text{ps}$) InGaAs photodetector

with the pump laser operating at 10kHz. Once located the CW seed beam ($\lambda_{seed}=1553\text{nm}$) was introduced and parametric amplification signal was detected. This signal was observed over a 40°C temperature range ($35\text{-}75^\circ\text{C}$) to locate the optimal operating crystal temperature. The pump laser was then adjusted to operate at the desired repetition frequency of 981Hz and the same experiment repeated in order to calculate the amplified pulse energies. At this frequency the $1.553\mu\text{m}$ amplified output pulses had energies of $5.3\mu\text{J}$, corresponding to a conversion efficiency of $\sim 5\%$ for pump pulse energies of $110\mu\text{J}$ and a single-pass gain of $\sim 3.10^5$ ($\sim 55\text{dB}$). Typical pulse bandwidths were around 2.1nm , corresponding to a coherence length of $\sim 1.1\text{mm}$. These values were used as the benchmark against which the operational performance of the two chirped OPAs was to be compared.

3. Axially chirped fs-seeded OPA

The initial experimental configuration for the axially chirped fs-seeded OPA used the same experimental setup as the CW-seeded system except for the crystal. Changing the crystal was trivial and the only other requirement was to modelock the Er:fibre laser to produce a broadband spectrum. Running CW, the seed spectrum had a bandwidth $\sim 2\text{nm}$ while running modelocked seed spectrum had a bandwidth in excess of 100nm ($1500\text{-}1600$).

In this mode the seed laser operated at a repetition frequency of 54.25MHz delivering pulses with energies of $\sim 18\text{pJ}$ ($\sim 1\text{mW}$ average power) in the horizontal polarisation state. Appropriate electronics were supplied with the seed laser (Menlosystems GmbH) to allow its exact operating frequency to be slaved to an external source (the pump lasers Q-switch master oscillator) and fine control was possible due to piezoelectric control of a free-space section of the seed laser cavity.

Consequently the repetition rates of the two lasers could be locked together to achieve high-quality synchronisation in their output timing. It was necessary to make optical path length adjustments to optimise the pump/seed pulse temporal overlap which was implemented by removing sections of the SMF28 stretching reel and monitoring the pump/seed temporal overlap using a fast InGaAs photodiode.

After synchronising the pump and seed pulses, the full device was configured and a parametric signal detected and optimised. The OPA signal was then monitored as a function of crystal temperature to locate the optimal crystal temperature corresponding to the seed spectral peak (1576nm). The optimal temperature was measured at 75°C where pulses with energies $\sim 100\text{nJ}$ were then recorded, indicating a gain of 37dB . This corresponds to a conversion efficiency of $\sim 0.08\%$, which was very low in comparison to the 5% observed for the CW-seeded unchirped OPA. Spectral measurements were then made of the parametric signals using a lock-in amplifier and a slow scanning-mirror assembly. Figure 3 shows the spectrum from the axially chirped OPA where a full-width-half-maximum (FWHM) bandwidth in excess of 80nm was measured corresponding to a coherence length of $\sim 31\mu\text{m}$ centred on 1576nm . This is a reduction in the coherence length by a factor of more than 35 times over the CW-seeded unchirped OPA.

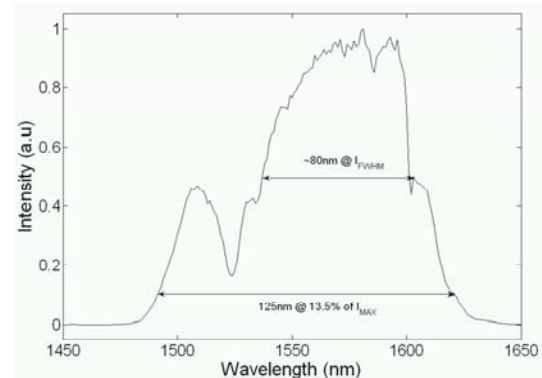


Fig.3: OPA spectrum measured at $T_c=100^\circ\text{C}$ showing a FWHM bandwidth of $\sim 80\text{nm}$.

Various strategies were implemented to attempt to boost the amplified pulse energies including more aggressive beam focusing geometries (elliptical changed to spherical) and the inclusion of an erbium-doped-fibre-amplifier (EDFA) to boost seed pulse energies. Altering the focal geometry increased the pump fluence from 0.175Jcm^{-1} to 0.85Jcm^{-1} which increased pulse energies to $2.55\mu\text{J}$. This corresponds to a gain of 51.5dB and a conversion efficiency of $\sim 2\%$ which was an increase of almost 2 orders of magnitude from the elliptical focusing arrangement. The inclusion of the EDFA did result in the stabilization in the parametric signal however no increase in pulse energy was measured. We concluded that despite its broad spectral bandwidth, the axially chirped OPA had insufficient power for use in even a short-range ($\sim 1\text{km}$) BIL system.

4. Laterally chirped fs-seeded OPA

By using a lateral chirp the gain-per-unit-frequency can be maximised, however this has the unwanted effect giving the different frequencies different paths through the crystal (i.e. creating spatial chirp). As a result, the spatial overlapping of the generated frequencies resulting from the axially chirped crystal is lost unless corrective measures are taken. This makes the setup more complex requiring two noticeable changes in the device configuration compared to the axially chirped setup. Firstly, to maximise the conversion bandwidth of the crystal the pump beam must fill as much of the grating aperture, which favours an elliptical pump beam profile. Secondly, to make best use of the bandwidth from the seed laser the component frequencies should only be directed into the correct region of the fan-out grating. This can be achieved by dispersing the seed beam prior to spherically focusing. This produces a line of frequency-dependent point foci matched to both the elliptical pump profile and

crystal grating period. Figure 4 shows the final experimental configuration that was used, highlighting the function of the extra steering optics and the dispersive prism needed to generate the necessary seed beam profile.

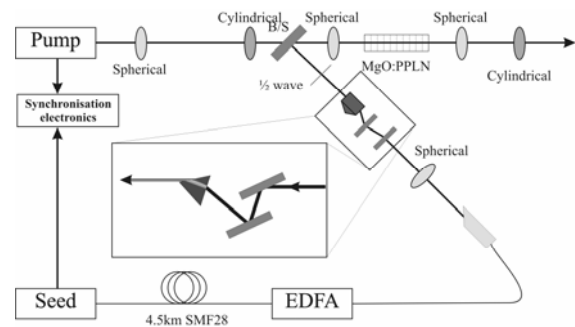


Fig.4: Schematic of the experimental configuration of the laterally chirped fs-seeded OPA.

The crystal itself contained 3 fan-out gratings each with different maximum fan angles and an aperture size of $0.5 \times 1.5\text{mm}$. The grating with the largest fan angle ($\sim 20^\circ$) contained the same level of chirp as found in the axially chirped crystal with a period that varied from $30.8\text{-}30.1\mu\text{m}$ in the vertical plane. As a result the pump beam was focused into the crystal using a 100mm cylindrical lens producing a collimated beam in the vertical plane with a waist size of 1mm and focused beam in the horizontal plane with a waist size of $\sim 170\mu\text{m}$. Limitations on the available materials for use as the dispersive medium in the seed arm resulted in the use of a non-optimal near equilateral prism of SF10. This material was able to sufficiently disperse the beam in the vertical plane to produce a collimated beam with a width of $300\mu\text{m}$. As a result, both the pump and seed beams were not fully optimised but were sufficiently matched to achieve operation. After careful configuration the detection of a parametric signal allowed performance of the conversion capabilities of the three gratings to be assessed as a function of crystal temperature. The grating with the lowest chirp ($30.35\text{-}30.55\mu\text{m}$) generated pulses with energies in excess of $4.2\mu\text{J}$, the next grating ($30.3\text{-}30.6\mu\text{m}$) generated pulses with energies of $5.35\mu\text{J}$ and the final

grating (30.1-30.8 μm) generated pulses with $\sim 3.5\mu\text{J}$ energies. All three gratings outperformed the axially chirped grating in terms of pulse energies, although the most chirped grating did not meet expectations. Preliminary spectral data implies bandwidth of between 10nm and 50nm but full data remains to be recorded.

This experiment is still ongoing and further data will be presented at the conference.

5. Q-switched Chirped OPO

The experimental setup for any OPO has a cavity around the crystal and hence a more complex optical arrangement however as it is self-seeding no seed source delivery section is needed. Due to the requirements of a Q-switched OPO the device has the potential to be very compact, only requiring pump collimation and then focusing into the cavity containing the chirped crystal. The main concern for this OPO was that the cavity mirrors be as close to the crystal as possible ensuring maximum exposure to the gain medium for the resonant pulses. Based on these requirements the OPO was initially configured to investigate the crystal properties without the use of a cavity. The device oscillated without the need for cavity mirrors due to end-facet coatings with high reflectivity at the idler wavelength, resulting in a very compact monolithic device. In preliminary work, power measurements indicate signal pulses with energies in excess of $25\mu\text{J}$ at 1kHz using $110\mu\text{J}$ pump pulses corresponding to a conversion efficiency of $\sim 23\%$. Spectra measured using the most chirped grating showed bandwidths in excess of 15nm which is more than a 50% increase when compared to spectra from the unchirped grating. Figure 5 shows a comparison between the spectral bandwidths generated by the gratings with no chirp and the maximum chirp using a spectrometer with a resolution of $\sim 3\text{nm}$.

At the time of writing this device is still

under investigation and further details will be presented at the conference.

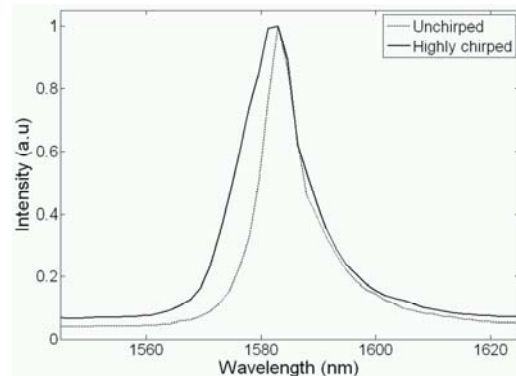


Fig.5: Two OPO spectra recorded at $T_c=145^\circ\text{C}$ using the unchirped grating (dotted line) and the highest chirped grating (solid line)

6. Conclusions

In conclusion we have demonstrated that chirped frequency conversion in broadband seeded optical parametrically amplifiers is a viable technique for enhancing the spectral bandwidth of coherent sources. Several different strategies were investigated with each showing different benefits and limitations. In terms of pulse energies the fan-out grating approach shows most promise and further investigations using a broader pump beam and a more dispersed seed beam would be useful in determining spectral bandwidth limitations. The OPO also shows significant promise in terms of pulse energies and an investigation into the maximum usable grating chirp would maximise the bandwidth enhancement available from this device although its compact size and high pulse energies already make it an attractive device for a range of applications.

7. References

1. D. A. Kleinman, *Phys. Rev.*, 1968. **174**(3): p. 1027-1041.
2. K. A. Tillman, et al, *J. Opt. Soc. Am. B-Opt. Phys.*, 2003. **20**(6): p. 1309-1316.
3. P. E. Powers, et al., *Opt. Lett.*, 1998. **23**(3): p. 159-161
4. D. A. Bryan, et al, *Appl. Phys. Lett.*, 1984. **44**(9): p. 847-849.
5. R. L. Byer, et al, *Appl. Phys. Lett.*, 1981. **39**(1): p. 17-19.
6. S. Guha, et al, *IEEE J. Quantum Electron.*, 1982. **18**(5): p. 907-912.